

Improved Ion-Diffusion Performance by Engineering Ordered Mesoporous Shell in Hollow Carbon Nanospheres

Jing Peng,^{a,b,†} Weicai Zhang,^{a,b,†} Peifeng Yu,^{a,b,†} Haibo Pang,^{a,b} Mingtao Zheng,^{a,b}

Hanwu Dong,^{a,b} Hang Hu,^{a,b} Yong Xiao,^{a,b} Yingliang Liu,^{a,b,*} Yeru Liang^{a,b,*}

^aCollege of Materials and Energy, Guangdong Provincial Engineering Technology Research Center for Optical Agriculture, South China Agricultural University, Guangzhou 510642, China

^bGuangdong Laboratory of Lingnan Modern Agriculture Science and Technology, Guangzhou 510642, China

Experimental section

Materials

Tetraethyl orthosilicate (Shanghai Chemical Reagent Factory, A.R.), 3-(methylacryloyl) propyltrimethoxysilane (Aladdin, A.R.), glutaraldehyde (Guangzhou Chemical Reagent Factory, 25%), ammonia water ($\text{NH}_3 \cdot \text{H}_2\text{O}$, Guangzhou Chemical Reagent Factory, 25%), phenol (Guanghua Chemical Reagent Factory, A.R.), hydrofluoric acid (HF, Guangzhou Chemical Reagent Factory, 40%), formaldehyde solution (37.5%, Guangdong Chemical Reagent Factory, A.R.), triblock copolymer F127 (Sigma-Aldrich, A.R.), 3-(trimethoxysilyl)propyl methacrylate (Aldrich, 97%), anhydrous aluminum chloride (Aldrich, 99.99%), and carbon tetrachloride (Tianjin Chemical Reagent Factory, A.R.) were used as received.

Synthesis of samples

Synthesis of functionalized SiO₂-CHO nanospheres. Typically, a mixed solution, including 20 mL of ethanol, 6 mL of deionized water and 4 mL of ammonia aqueous solution, was configured and named as solution A. In addition, 1.7 mL of tetraethyl orthosilicate was mixed with 30 mL of ethanol, which is solution B. Then, solution B was added to solution A immediately under stirring. After stirring at 26 °C for 5 h, 0.15% (volume ratio) of 3-(methacryloxy) propyltrimethoxysilane ethanol solution was dropped into the above reaction solution. The mixture was continuously stirred for 48 h at room temperature. After centrifugation with ethanol for several times, the amine-terminated SiO₂-NH₂ nanoparticles were acquired. Subsequently, the SiO₂-NH₂ nanoparticles were redispersed in 150 mL of ethanol and 2 mL of 25% glutaraldehyde aqueous solution. After stirring the solution for 2 h at 80 °C, the aldehyde-terminated SiO₂-CHO nanoparticles were collected by centrifugation with water and ethanol for several times.

Synthesis of resol-F127 composite solution. Typically, 0.61 g of phenol and 15 mL of NaOH aqueous solution (0.1 mol L⁻¹) was mixed under stirring. Then, additional 2.1 mL of formaldehyde solution (37 wt.%) were added. After that, the limpid mixture was reacted at 70 °C for 0.5 h under stirring and then was cooled to 26 °C to harvest phenolic resols. Immediately, the obtained phenolic resols was mixed with aqueous solution of triblock copolymer F127. After stirring the resultant mixture continuously at 65 °C for 13 h with a stirring speed of 340 ± 5 rpm, the resol-F127 composite solution was obtained.

Synthesis of hollow ordered mesoporous carbon nanospheres. Typically, 40 mL of the aforementioned resol-F127 composite solution was measured by volumetric cylinder. 0.30 g of SiO₂-CHO nanoparticles were evenly distributed in 150 mL of deionized water as well. The two solutions were mixed and stirred steady at 65 °C for 6 h with a stirring speed of 400 ± 5 rpm. After that, the acquired solution was transformed to a stainless steel autoclave. And the hydrothermal temperature was strictly controlled at 130 °C and last for 24 h. After centrifugation with water and ethanol for several times, the as-prepared SiO₂@polymer nanospheres were carbonized in the N₂ atmosphere at 800 °C for 3 h, in which the heating rate was 1 °C min⁻¹ when the carbonization temperature below 600 °C and turned to 5 °C min⁻¹ in the range of 600-800 °C. Then HF aqueous solution was added to the resulting SiO₂@ordered mesoporous carbon nanocomposite to remove SiO₂. After washed by deionized water for several times, hollow ordered mesoporous carbon nanospheres were successfully synthesized. For comparison, a control sample was also prepared. Its preparation procedure was exactly the same as that of the hollow ordered mesoporous carbon nanospheres except that the rare SiO₂ nanospheres were employed as template.

Preparation of hollow disordered microporous carbon nanospheres. Hollow disordered microporous carbon nanospheres were synthesized following the procedure reported previously^[1]. Typically, SiO₂ nanospheres with a diameter of about 120 nm were prepared based on a Stöber method. After that, a solution of 3-(trimethoxysilyl)propyl methacrylate (2.25 mL) in ethanol (100 mL) was then

dropped into the dispersion of the above SiO₂ nanospheres solution under stirring at 30 °C for 36 h. After centrifugation, washed and dried, the functionalized SiO₂ nanospheres were obtained. Subsequently, the styrene-divinylbenzene copolymer shells were coated onto these functionalized SiO₂ nanoparticles through an emulsion copolymerization reaction. Afterwards, the hypercrosslinking of 1.0 g of SiO₂@PS nanospheres was carried out after adding the mixture of anhydrous aluminum chloride (2.8 g) and carbon tetrachloride (60 mL) under stirring for 24 h, resulting in the core-shell structured SiO₂@xPS nanospheres. The as-prepared SiO₂@xPS nanospheres were carbonized at 900 °C for 3 h in N₂ flow. After using HF to remove the silica core, the hollow disordered microporous carbon nanospheres were obtained.

Structural characterization

The microstructure of the samples was observed with a FEI Tecnai G2 Spirit transmission electron microscope (TEM) coupled with Energy Dispersive X-ray Spectroscopy and a JSM-6330F scanning electron microscope (SEM). About 50-100 nanoparticles were selected at random in a SEM or TEM image to get a statistical analysis of the particle size distribution. The maximum value in the obtained particle size distribution curve was related to as the diameter of nanoparticles. A D-MAX 2200 VPC diffractometer with Cu K α radiation ($\lambda = 1.5418 \text{ \AA}$) was used to examine X-ray diffraction measurements. Nitrogen adsorption/desorption measurements were analyzed by a Micromeritics ASAP 2020 analyzer at 77K. The surface area was calculated by Brunauer-Emmett-Teller (BET) theory. The original density functional theory integrated with non-negative regularization provides an excellent basis to

calculate the aperture distribution. According to the amount absorbed at P/P_0 of about 0.99, the total pore volume was successfully inferred.

Electrochemical tests

The working electrodes were made up of binder (*i.e.*, polytetrafluoroethylene) and active material with a mass ratio of 8:92. The obtained mixture was rolled into flakes after the volatilization of solvent. Immediately, the flakes were cut into several certain area small pieces with a diameter of 12 mm and pressed with nickel foam by hydraulic press, in which nickel foam was served as current collector. After that, the electrode piece was dried to constant weight and the mass of carbon sample on the electrode piece was calculated. The average loading mass of each electrode piece is about 8 mg per piece. 6 M KOH aqueous solution was used as the electrolyte. Two electrodes with the similar mass were assembled with a fibrous paper separator. The cyclic voltammetry (CV) curves were measured by CHI 760e electrochemical workstation. The capacitances of electrodes were calculated from galvanostatic charge-discharge (GCD) curves by using the equation as following:

$$C = \frac{2 \times I \times \Delta t}{A \times \Delta U}$$

in which I (A), Δt (s), and ΔU (V) stand for constant current, discharge time of GCD curves, and discharge voltage excluding the IR drop, respectively. C ($\mu\text{F cm}^{-2}$) corresponds to areal capacitance of electrode materials. A (cm^2) represents the area of electrode slices.

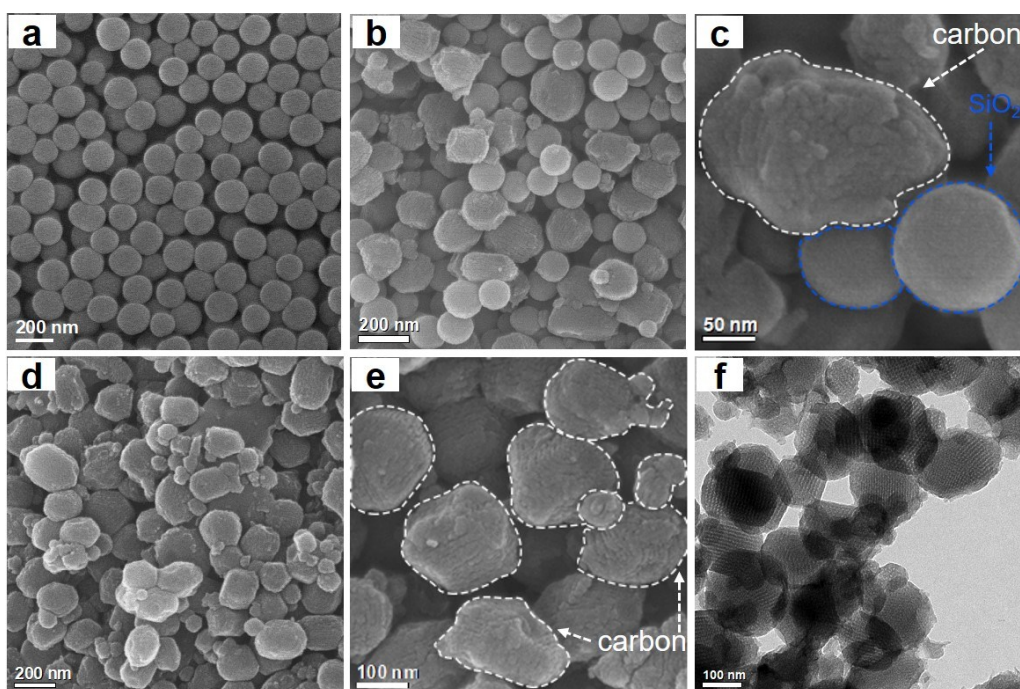


Fig. S1 SEM images of (a) SiO₂ nanospheres, (b, c) SiO₂/carbon composites and (d, e) solid carbon nanoparticles, (f) TEM image of solid carbon nanoparticles.

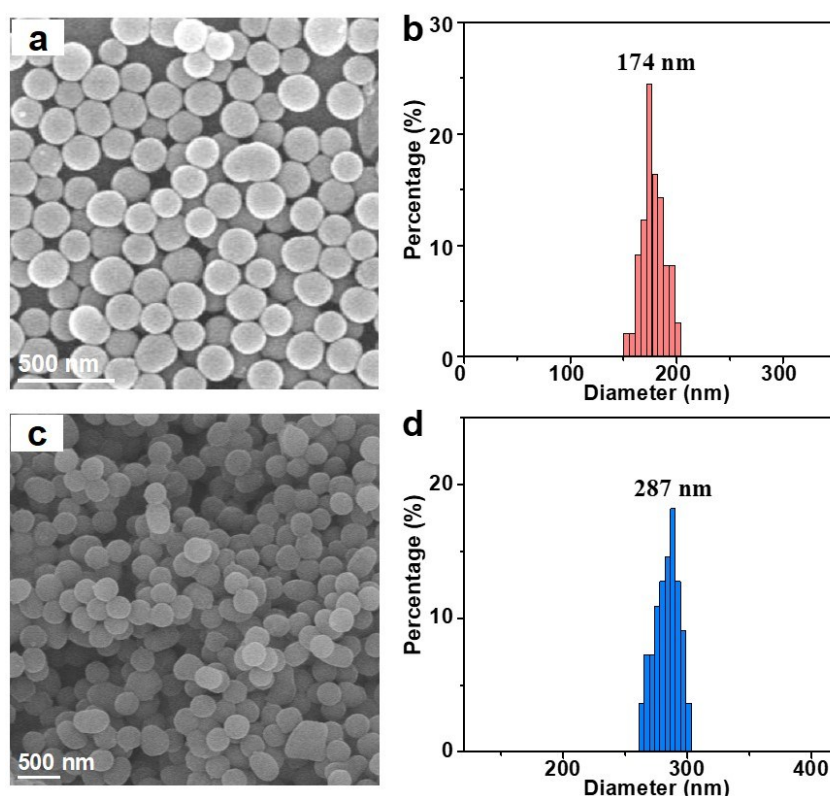


Fig. S2 (a) SEM image and (b) particle size distribution of SiO₂-CHO nanospheres. (c) SEM image and (d) particle size distribution of SiO₂@polymer nanospheres.

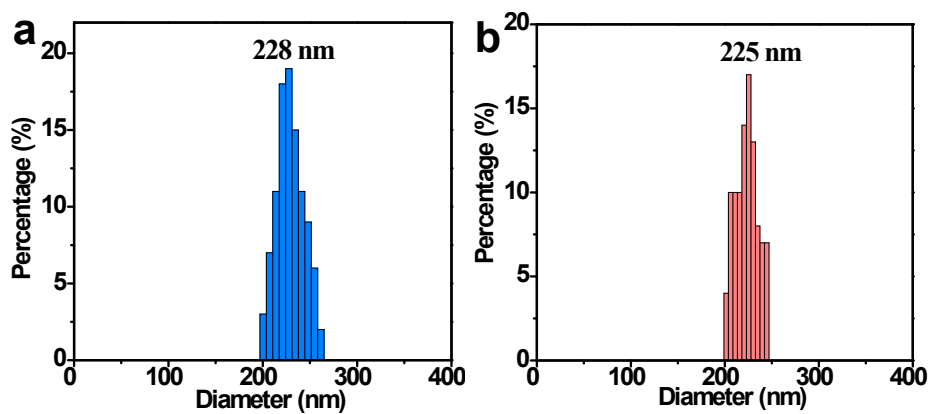


Fig. S3 Particle size distribution of (a) SiO₂@OMCNSs and (b) HOMCNSs.

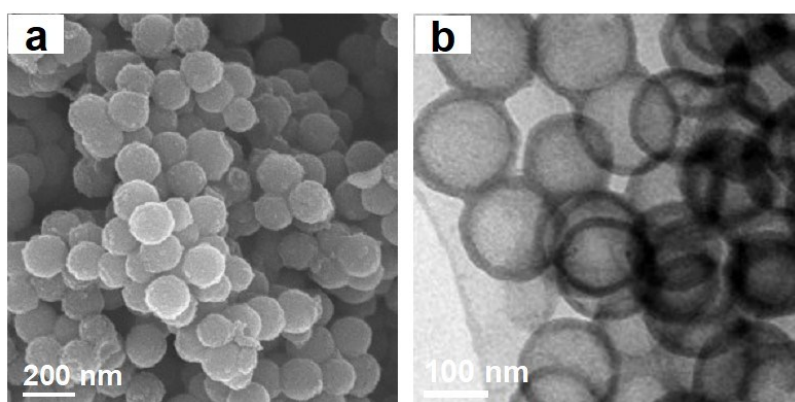


Fig. S4 (a) SEM and (b) TEM images of HDMCNSs.

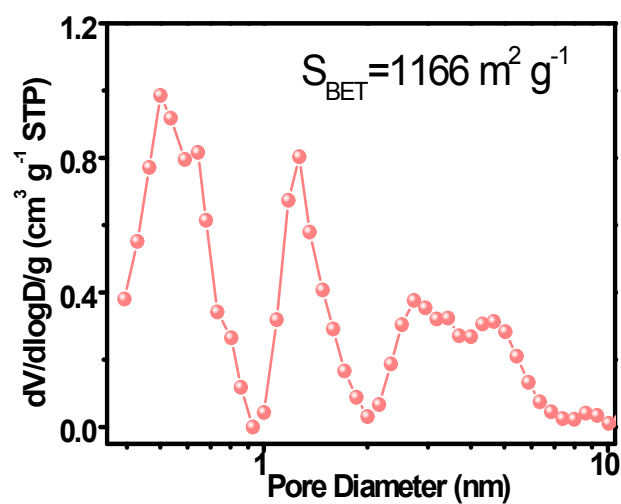


Fig. S5 Pore size distribution curve and the BET surface area of HDMCNSs.

Table S1 Comparison of specific capacitances per surface area among HOMCNSs, HDMCNSs and typical carbon materials reported in the literatures.

References	BET surface area ($\text{m}^2 \text{g}^{-1}$)	Specific capacitance per surface area ($\mu\text{F cm}^{-2}$)	Current density
This work	502 (HOMCNSs)	16.13	0.1 A g^{-1}
		13.94	1 A g^{-1}
		13.65	2 A g^{-1}
	1166 (HDMCNSs)	12.32	0.1 A g^{-1}
		8.26	1 A g^{-1}
		6.24	2 A g^{-1}
Ref. [2]	3003	7.99	0.5 A g^{-1}
Ref. [3]	2435	8.09	0.2 A g^{-1}
Ref. [4]	3496	9.67	2 mV s^{-1}
Ref. [5]	1416	9.75	0.2 A g^{-1}
Ref. [6]	1785	11.20	0.1 A g^{-1}
Ref. [7]	2841	11.62	1 A g^{-1}
Ref. [8]	1681	12.02	5 mV s^{-1}
Ref. [9]	2959	8.79	0.6 A g^{-1}
Ref. [10]	2509	12.40	0.25 A g^{-1}
Ref. [11]	3199	8.03	1 A g^{-1}
Ref. [12]	2502	9.19	1 A g^{-1}
Ref. [13]	2340	11.97	0.1 A g^{-1}

References

- [1] L. Chen, Y. Liang, H. Liu, W. Mai, Z. Lin, H. Xu, R. Fu and D. Wu, *RSC Adv.*, 2016, 6, 49661-49667.
- [2] H. T. Zhang, L. Zhang, J. Chen, H. Su, F. Y. Liu and W. Q. Yang, *J. Power Sources*, 2016, 315, 120-126.
- [3] P. Hao, Z. H. Zhao, Y. H. Leng, J. Tian, Y. H. Sang, R. I. Boughton, C. P. Wong, H. Liu and B. Yang, *Nano Energy*, 2015, 15, 9-23.
- [4] Y. H. Hu, H. B. Wang, L. F. Yang, X. R. Liu, B. Zhang, Y. L. Liu, Y. Xiao, M. T. Zheng, B. F. Lei, H. R. Zhang and H. G. Fu, *J. Electrochem. Soc.*, 2013, 160, H321-H326.
- [5] W. J. Si, X. Z. Wu, W. Xing, J. Zhou and S. P. Zhuo, *J. Inorg. Mater.*, 2011, 26, 107-112.
- [6] Y. Y. Wang, B. H. Hou, H. Y. Lu, F. Wan, J. Wang and X. L. Wu, *RSC Adv.*, 2015, 5, 97427-97434.
- [7] C. Peng, X. B. Yan, R. T. Wang, J. W. Lang, Y. J. Ou and Q. J. Xue, *Electrochim. Acta*, 2013, 87, 401-408.
- [8] J. Sodtipinta, C. Ieosakulrat, N. Poonyayant, P. Kidkhunthod, N. Chanlek, T. Amornsakchai and P. Pakawatpanurut, *Ind. Crop. Prod.*, 2017, 104, 13-20.
- [9] H. Jin, X. M. Wang, Z. R. Gu and J. Polin, *J. Power Sources*, 2013, 236, 285-292.
- [10] X. A. Li, W. Xing, S. P. Zhuo, J. Zhou, F. Li, S. Z. Qiao and G. Q. Lu, *Bioresour. Technol.*, 2011, 102, 1118-1123.
- [11] M. S. Balathanigaimani, W. G. Shim, M. J. Lee, C. Kim, J. W. Lee and H. Moon, *Electrochem. Commun.*, 2008, 10, 868-871.
- [12] Y. Fan, X. Yang, B. Zhu, P. F. Liu and H. T. Lu, *J. Power Sources*, 2014, 268, 584-590.
- [13] C. W. Wang, M. J. O'Connell and C. K. Chan, *ACS Appl. Mater. Interfaces*, 2015, 7, 8952-8960.